Available online at www.sciencedirect.com
SCIENCE DIRECT®
Biochemical and Biophysical Research Communications 306 (2003) 177–185
BBRC
www.elsevier.com/locate/ybbrc

Transmembrane segment 5 of the dipeptide transporter hPepT1 forms a part of the substrate translocation pathway

Ashutosh A. Kulkarni,[a] Ian S. Haworth,[a] and Vincent H.L. Lee[a,b,*]

[a] *Department of Pharmaceutical Sciences, University of Southern California, Los Angeles, CA 90089-9121, USA*
[b] *Department of Ophthalmology, University of Southern California, Los Angeles, CA 90089-9121, USA*

Received 20 April 2003

Abstract

This study is the first systematic attempt to investigate the role of transmembrane segment 5 of hPepT1, the most conserved segment across different species, in forming a part of the aqueous substrate translocation pathway. We used cysteine-scanning mutagenesis in conjunction with the sulfhydryl-specific reagents, MTSEA and MTSET. Neither of these reagents reduced wild-type-hPepT1 transport activity in HEK293 cells and *Xenopus* oocytes. Twenty-one single cysteine mutations in hPepT1 were created by replacing each residue within TMS5 with a cysteine. HEK293 cells were then transfected with each mutated protein and the steady-state protein level, [^{3}H]Gly-Sar uptake activity, and sensitivity to the MTS reagents were measured. S164C-, L168C-, G173C-, and I179C-hPepT1 were not expressed on the plasma membrane. Y167C-, N171C-, and S174C-hPepT1 showed $\leqslant$25% Gly-Sar uptake when compared with WT-hPepT1. P182C-hPepT1 showed $\sim$40% specific activity whereas all the remaining transporters, although still sensitive to single cysteine mutations, exhibited more than 50% specific activity when compared to WT-hPepT1. The activity of F166C-, L176C-, S177C-, T178C-, I180C-, T181C-, and P182C-hPepT1 was partially inhibited, while the activity of F163C- and I170C-hPepT1 was completely inhibited by 2.5 mM MTSEA. F163C, I165C, F166C, A169C, I170C, S177C, T181C, and P182C were clearly accessible to 1 mM MTSET. Overall, these results suggest that TMS5 lines the putative aqueous channel and is slightly tilted from the vertical axis of the channel, with the exofacial half forming a classical amphipathic α-helix and the cytoplasmic half being highly solvent accessible.

Keywords: Cysteine-scanning; Dipeptide; Transporter; MTS; Transmembrane segment; PepT1; Mutagenesis

The mammalian intestinal dipeptide transporter hPepT1, located on the apical membrane of the intestinal epithelial cells, is responsible for the absorption of di- and tripeptides from the intestinal tract after peptide release by enzymatic breakdown of dietary or endogenous proteins [1,2]. Additionally, active transport mediated by hPepT1 is responsible for the high bioavailability of orally active peptide-based drugs such as β-lactam antibiotics [3,4], angiotensin converting enzyme inhibitors [5,6], and anticancer drugs like bestatin [7]. Many non-peptidic compounds have also been shown to be substrates for PepT1 [8,9]. This absorption is proton coupled, driving protons and the substrate down an electrochemical proton gradient. Liang et al. [10] have successfully cloned the cDNA encoding the transporter. On the basis of the cDNA sequence and a hydropathy calculation, hPepT1 is predicted to have 708 amino acids and 12 transmembrane segments (TMS) [10]. Seven of the 12 putative transmembrane segments (segments 1, 3, 5, 7, 8, 9, and 10) are predicted to be amphipathic α-helices.

PepT1 is a very lucrative target for the development of prodrugs because of its broad substrate specificity and high capacity. L-Valacyclovir, an orally active prodrug of the antiviral drug acyclovir, has been shown to be a substrate for PepT1 [11,12]. In order to facilitate rational design of drugs and prodrugs for this transporter, it is essential to elucidate the nature of its substrate-binding site and mechanism of transport. This has led to an increased focus on delineating the structure–

* Corresponding author. Fax: 1-323-442-1390.
E-mail address: vincentL@usc.edu (V.H.L. Lee).

0006-291X/03/$ - see front matter © 2003 Elsevier Science (USA). All rights reserved.
doi:10.1016/S0006-291X(03)00926-4

function relationships of PepT1. Since direct structural approaches (crystallization, structural characterization by NMR or other spectroscopic methods) to transmembrane proteins are limited, direct characterization of the binding site and translocation conduit will probably not be available soon.

The substituted cysteine accessibility method (SCAM) has made it possible to study the fine structure of various ion channels and transporters. In particular, the portion of transmembrane segments lining the channel pore or the solute pathway can be identified by determining the amino acid positions that are accessible to water-soluble cysteine modifying reagents [13–16]. This method has been applied for various membrane proteins including the lactose permease of *Escherichia coli* [13], dopamine D2 receptor [17,18], Glut1 glucose transporter [19], glutamate transporter gltT [20], and Tn10 encoded metal-tetracycline/H^+ antiporter [21].

In this study we used cysteine-scanning mutagenesis in conjunction with sulfhydryl-specific chemical reagents to directly address the role of transmembrane segment 5 in forming the hPepT1 substrate translocation pathway. We chose transmembrane segment 5 for the following reasons: (1) TMS5 is one of the amphipathic transmembrane segments that has been proposed to line the substrate translocation pathway [22]. (2) An important role for tyrosine 167 (Y167) in TMS5 in the modulation of dipeptide transport by hPepT1 was predicted by computer modeling and subsequently confirmed by site-directed mutagenesis [23]. (3) To further investigate the obligatory role of Y167, site-directed mutagenesis was used to generate Y167F-, Y167H-, and Y167S-hPepT1 mutations. None of these mutations restored the transport function of hPepT1, suggesting a strategic role for Y167 in hPepT1 function in terms of the chemical and spatial properties of its phenolic group [23,24]. Our results provide the first experimental evidence suggesting that TMS5 lines the putative aqueous channel and is slightly tilted from the vertical axis of the channel, with the exofacial half forming a classical amphipathic α-helix and the cytoplasmic half being highly solvent accessible.

Materials and methods

Materials. [^{3}H]Glycyl-sarcosine (4 Ci/mmol) was purchased from Moravek Chemical (Brea, CA). Cell culture media and supplies were obtained from Gibco (Grand Island, NY). 2-Aminoethyl methanethiosulfonate hydrobromide (MTSEA) and [2-(trimethylammonium) ethyl]methanethiosulfonate bromide (MTSET) were purchased from Toronto Research Chemicals (Toronto, Ont.). All chemicals were of the highest purity available commercially.

Site-directed mutagenesis. The hPepT1 cDNA (kindly provided by Dr. Matthias A. Hediger) was subcloned into the eukaryotic expression plasmid pcDNA3 (Invitrogen, Carlsbad, CA) by ligating the 2306 *Kpn*I/*Bam*HI fragment into the multiple cloning sites of pcDNA3. This pcDNA3-hPepT1 plasmid is under the control of cytomegalovirus (CMV) promoter. This plasmid was used as a template for all the mutagenesis reactions. The standard site-directed mutagenesis protocol provided by the manufacturer was followed using the Gene Editor site-directed mutagenesis kit (Promega, Madison, WI). The mutated cDNA was transformed into an *E. coli* strain, BMH71-18 Mut.S, which is incapable of correcting mismatches. This process of amplification was repeated once more using the JM109 competent cells to enrich the mutated population. The transformed cells were then plated onto ampicillin LB plates and incubated overnight. Individual colonies obtained on the ampicillin LB plates were amplified further. The plasmid extracted from each colony was then subjected to DNA sequencing analysis to verify the mutations (Genemed Synthesis, San Francisco, CA).

Transient transfection of the mutants in HEK293 cells. The HEK293 cells were split into 60 × 15 mm dishes and grown overnight (>20 h) at 50–75% confluence. The medium was then removed and 2 ml transfection solution (2 ml DMEM with 20 μl DEAE-dextran (25 mg/ml) and 10 μl chloroquine (20 mM)) was added to each dish. The mixture was then incubated at 37 °C for 2 h. The transfection solution was previously prepared in a stock of 20 ml which was then divided into 10 portions (2 ml each), 1 μg of DNA was added to each portion, and the mix was incubated at 37 °C for 10 min. After removing the transfection solution, 2 ml of 10% DMSO in DPBS (sterile PBS) was added to each dish. Following an incubation period of 2 min at room temperature, the DMSO solution was removed and replaced by 4 ml fresh DMEM in each dish. The cells were grown overnight and on the following day, each dish was split into six wells of 12-well plates. Immunolocalization and uptake experiments were performed 48 h after splitting.

Immunolocalization. The procedure for immunofluorescence microscopy staining has been described in detail previously [23]. Briefly, transfected HEK293 cells were plated onto coverslips and cultured for 48 h. The coverslips were then incubated with 3.7% formaldehyde in phosphate buffered saline (PBS) at room temperature for 20 min. After washing thrice with PBS, the coverslips were permeabilized with 0.5% Triton X-100 for 15 min, washed once, and then blocked with 1% bovine serum in PBS at room temperature for 30 min. After washing once with 0.05% Tween 20 in PBS (PBST), the coverslips were incubated with the primary antibody (antibody against the intracellular C-terminus of hPepT1) for 2 h. After washing thrice with PBST, they were incubated with FITC-conjugated secondary antibody for 1 h. The coverslips were washed again with PBST (twice) and PBS (once). Finally, the coverslips were mounted onto slides with anti-fade medium and examined by fluorescence microscopy.

Inhibition studies with sulfhydryl reagents. Prior to the uptake measurements, the transfected cells, adhered to the wells, were washed with the transport medium (Mes–Tris, pH 6, buffer). Each well was then incubated for 10 min at 37 °C with a solution containing [^{3}H]Gly-Sar (0.5 μCi/ml) after pre-incubation with 2.5 mM MTSEA or 1 mM MTSET (Toronto Research Chemicals, Ont., Canada) for 10 min. After washing thrice in ice-cold Mes–Tris (pH 6.0) buffer, the cells were lysed in 1 ml lysis buffer (1% SDS). BCA protein assay reagents were used to determine the protein content of each well and the cell-associated radioactivity was measured in a Beckman liquid scintillation counter.

Computational analysis. A helical wheel model of the transmembrane segment 5 of hPepT1 was constructed using the Lasergene software (DNASTAR, Madison, WI). The three-dimensional models were generated using in-house software (TMD) and viewed using WebLab ViewerPro 3.7 (Accelrys, San Diego, CA).

Results

Wild-type hPepT1 contains 11 endogenous cysteines (five in the transmembrane segments, three in the intracellular loops, and three in the extracellular loops).

However, WT-hPepT1 expressed in HEK293 cells retained ~85% of its uptake activity when treated with either 2.5 mM MTSEA or 1 mM MTSET. This suggests that either these endogenous cysteines are not reactive to the MTS reagents or that their modification does not have a significant impact on the transport activity of hPepT1. In order to further confirm this result, we expressed WT-hPepT1 in another heterogeneous system, *Xenopus* oocytes. As shown in Fig. 1, 1–100 μM MTSEA at pH 5.0 did not have any significant inhibitory effect on 20 mM Gly-Sar induced currents in these oocytes under voltage clamp conditions (holding potential: negative 70 mV).

We then used wild-type hPepT1 cDNA to construct the cysteine-scanning mutants for TMS5. Each of the 21 residues within TMS5 was individually mutated to a cysteine (Table 1). Mutated cDNAs were transiently transfected into HEK293 cells and the expression of the corresponding mutated transporter proteins was evaluated by immunofluorescence microscopy staining. Four out of the 21 mutated transporters (S164C-, L168C-, G173C-, and I179C-hPepT1) showed negligible expression on the plasma membrane of HEK293 cells 72 h post-transfection. This can be seen as a lack of fluorescence intensity at the edge of each cell (Fig. 2). As a result, HEK293 cells transfected with these mutated transporters showed negligible Gly-Sar uptake.

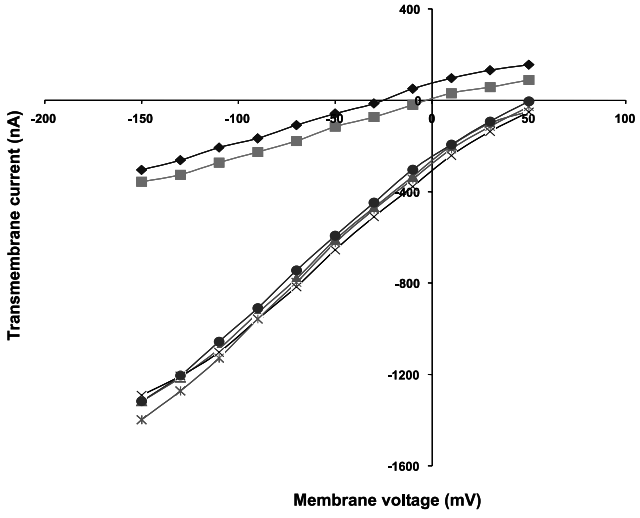

Fig. 1. Effect of 1–100 μM MTSEA on the transport activity of hPepT1. Voltage dependent transmembrane currents evoked by 20 mM Gly-Sar at pH 5.0 in oocytes expressing WT-hPepT1. Oocytes expressing WT-hPepT1 were pre-incubated with varying concentrations of MTSEA (1–100 μM) and then voltage was clamped at −70 mV holding potential. For determination of I/V (current/membrane potential) relationships, step changes in membrane potential (V_m) were applied from +50 to −150 mV in 20 mV increments, each for a duration of 100 ms using a voltage clamp amplifier (OC-725) controlled by a computer software program pCLAMP 8.1. Data are presented as I/V relationship for one oocyte and were reproduced in another oocyte. Treatments include: pH 7.4 perfusion buffer (◆); pH 5.0 perfusion buffer (■); and 20 mM Gly-Sar at pH 5.0 (▲); 20 mM Gly-Sar at pH 5.0 in the presence of 1 μM MTSEA (×), 10 μM MTSEA (*), and 100 μM MTSEA (●).

Table 1
Cysteine-scanning mutants of TMS5

Mutation	Codon change
Wild-type	NA
F163C	TTT to TGT
S164C	TCC to TGC
I165C	ATC to TGC
F166C	TTT to TGT
Y167C	TAC to TGC
L168C	TTG to TGC
A169C	GCT to TGT
I170C	ATT to TGT
N171C	AAT to TGT
A172C	GCT to TGT
G173C	GGA to TGC
S174C	AGT to TGT
L175C	TTG to TGC
L176C	CTT to TGT
S177C	TCC to TGC
T178C	ACA to TGC
I179C	ATC to TGC
I180C	ATC to TGC
T181C	ACA to TGC
P182C	CCC to TGC
M183C	ATG to TGC

A series of 21-cysteine-scanning mutant cDNAs was created by oligonucleotide-mediated site-directed mutagenesis of the wild-type hPepT1 cDNA. Each of the 21 amino acid residues within the putative transmembrane helix 5 was individually mutated to a cysteine. Amino acids are designated by single-letter code. For example, F163C represents the mutation of a phenylalanine at position 163 to a cysteine.

The remaining 17 mutated transporter proteins showed membrane expression comparable to the wild-type transporter (Fig. 2). Four out of these 17 mutated transporters (I165C-, L175C-, I180C-, and M183C-hPepT1) exhibited specific Gly-Sar uptake activities comparable to WT-hPepT1 (Fig. 3). Three mutated transporters (Y167C-, N171C-, and S174C-hPepT1) showed ⩽25% specific activity when compared to WT-hPepT1. P182C-hPepT1 showed ~40% specific activity whereas all the remaining transporters, although still sensitive to single cysteine mutations, exhibited more than 50% specific activity when compared to WT-hPepT1 (Fig. 3).

To determine the transmembrane residues that may comprise part of the substrate translocation pathway, we assessed the solvent accessibility of the cysteine residue in each of the 17 mutated transporter proteins. This was achieved by measuring the specific uptake activities of the mutated transporters after incubation with the sulfhydryl-specific chemical reagents, MTSEA (2.5 mM) and MTSET (1mM). Both reagents are soluble in aqueous solution, but MTSEA is also somewhat membrane-permeable with a molecular volume of 66 $Å^3$ whereas MTSET is essentially membrane-impermeable with a molecular volume of 109 $Å^3$. The uptake activities

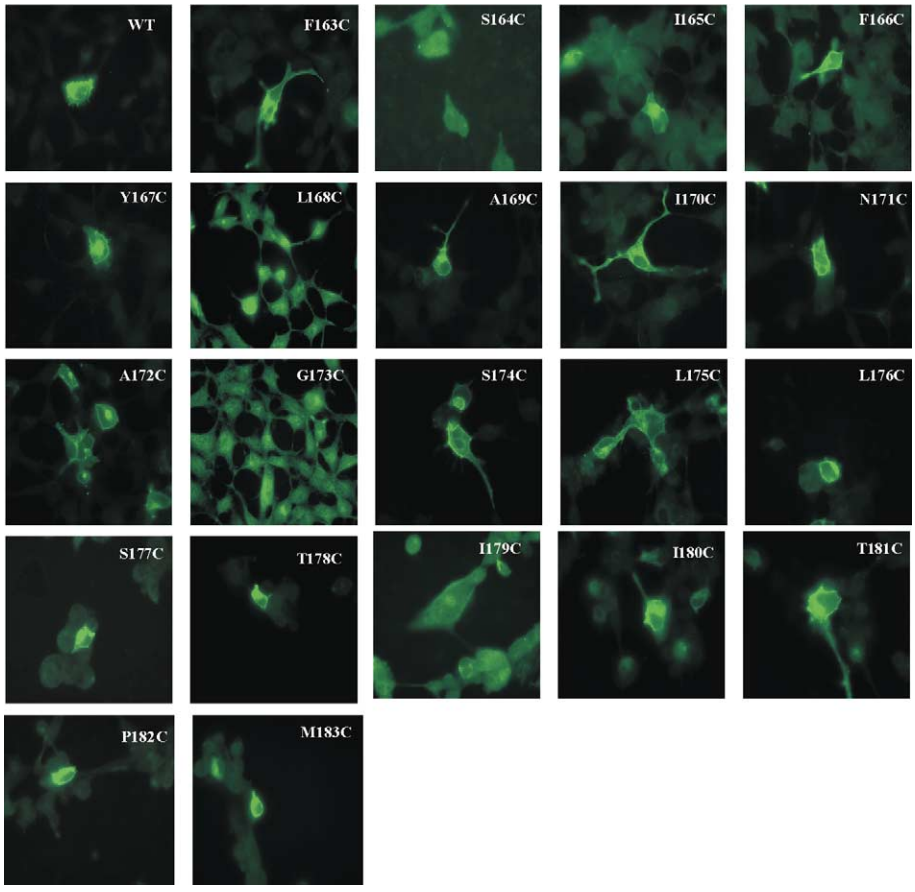

Fig. 2. Membrane localization of mutant hPepT1 transporter proteins in transiently transfected HEK293 cells. Seventy-two hours post-transfection, HEK293 cells were subjected to immunofluorescence microscopy using affinity purified rabbit anti-hPepT1 primary antibody and FITC conjugated secondary antibody, both at a dilution of 1:500. Immunostaining in wild-type hPepT1 transfected cells (WT) is shown as a positive control.

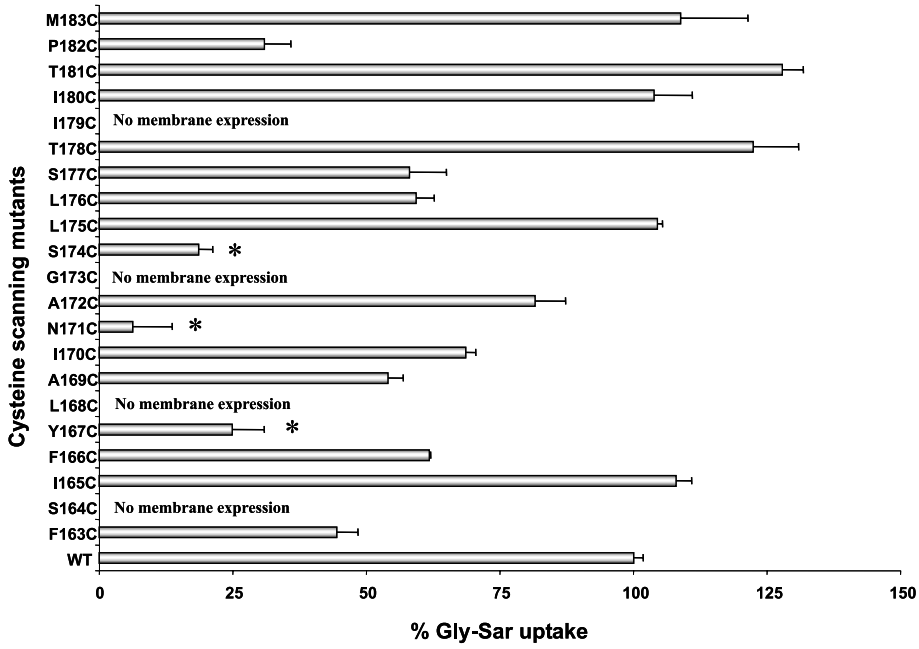

Fig. 3. Percentage Gly-Sar uptake activities of the cysteine-scanning mutants of TMS5 of hPepT1. [^{3}H]Gly-Sar uptake (0.5 μCi/ml, 10 min at 37 °C) was measured 72 h post-transfection in HEK293 cells, individually transfected with the cysteine-scanning mutants of TMS5 of hPepT1. Results represent the % Gly-Sar uptake of individual mutant transporter protein when compared with wild-type hPepT1 ($n = 4$–6). The background uptake values of mock-transfected HEK293 cells were subtracted. *, ⩽25% specific activity.

were compared to those measured in the presence of vehicle alone (Figs. 4 and 5).

The most dramatic reduction in Gly-Sar uptake ($p < 0.05$) after preincubation with 2.5 mM MTSEA was observed for single cysteine mutations at F163 and I170 (Fig. 4). F166C, L176C, S177C, T178C, I180C, T181C, and P182C also reacted with the 2.5 mM MTSEA, resulting in a decrease in uptake activity of these mutated proteins, but to a much lesser extent. This suggested that the amino acid side chains at these positions also reacted with the MTSEA reagent and therefore must be accessible from the external aqueous solvent. Even though cysteine substitutions at I165 and A172 showed a significant decrease in Gly-Sar uptake, this was considered to be inconsequential because the specific activities of these mutated transporters after incubation with 2.5 mM MTSEA were quite similar to that of WT-hPepT1 under similar conditions.

Preincubation with 1mM MTSET resulted in a drastic reduction in Gly-Sar uptake ($p < 0.05$) by the F163C-, I165C-, F166C-, A169C-, I170C-, S177C-, T181C-, and P182C-hPepT1 transporters (Fig. 5). This inhibition of Gly-Sar uptake was not partial as seen with the MTSEA reagent, but was complete and highly significant. There was an ~35% ($p < 0.05$) increase in the activity of T178C-hPepT1 after preincubation with 1 mM MTSET. Since the inherent activity of Y167C-, N171C-, and S174C-hPepT1 was very low (⩽25%), no significant difference in their activities was observed after incubation with either 2.5 mM MTSEA or 1 mM MTSET.

Discussion

To determine the role of TMS5 in hPepT1 transport activity, we performed exhaustive mutagenesis of all 21 of the TMS5 amino acids to cysteine followed by SCAM analysis. Immunostaining experiments performed to check the expression of all the mutated transporters on the plasma membrane of HEK293 cells showed that 4 out of the 21 mutated transporters (S164C-, L168C-, G173C-, and I179C-hPepT1) had negligible expression on the plasma membrane of HEK293 cells 72 h post-transfection. This can be seen as a lack of fluorescence intensity at the edge of each cell (Fig. 2). This suggested that single cysteine mutations at these amino acid positions were responsible for incorrect packaging and/or

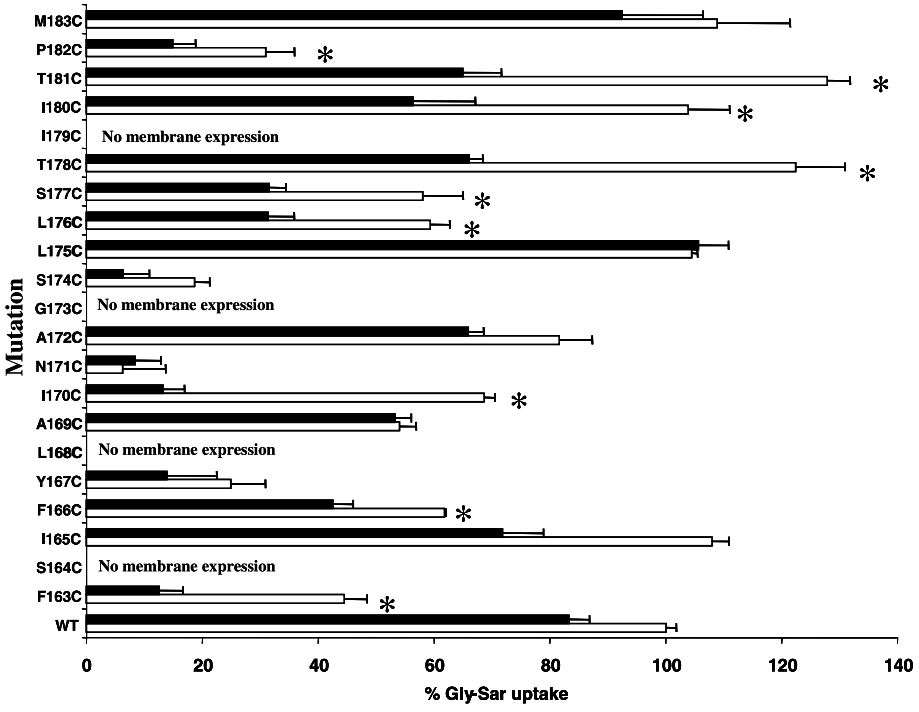

Fig. 4. Effect of 2.5 mM MTSEA on [^{3}H]Gly-Sar uptake activities of the cysteine-scanning mutants of TMS5 of hPepT1. Seventy-two hours post-transfection, the transfected cells, adhered to the wells, were washed with the transport medium (Mes–Tris, pH 6, buffer). Each well was then incubated for 10 min at 37 °C with a solution containing [^{3}H]Gly-Sar (0.5 μCi/ml) after pre-incubation with 2.5 mM MTSEA for 10 min. After washing thrice in ice-cold Mes–Tris (pH 6.0) buffer, the cells were lysed in 1 ml lysis buffer (1% SDS). BCA protein assay reagents were used to determine the protein content of each well and the cell-associated radioactivity was measured in a Beckman liquid scintillation counter. Results represent the % Gly-Sar uptake of each individual mutant transporter protein when compared with wild-type hPepT1 ($n = 4$–6). The background uptake values of mock-transfected HEK293 cells were subtracted. The white bars represent uptake activities in the absence of 2.5 mM MTSEA and the black bars represent uptake activities in the presence of 2.5 mM MTSEA. *, Highly significant inhibition of uptake activity by 2.5 mM MTSEA.

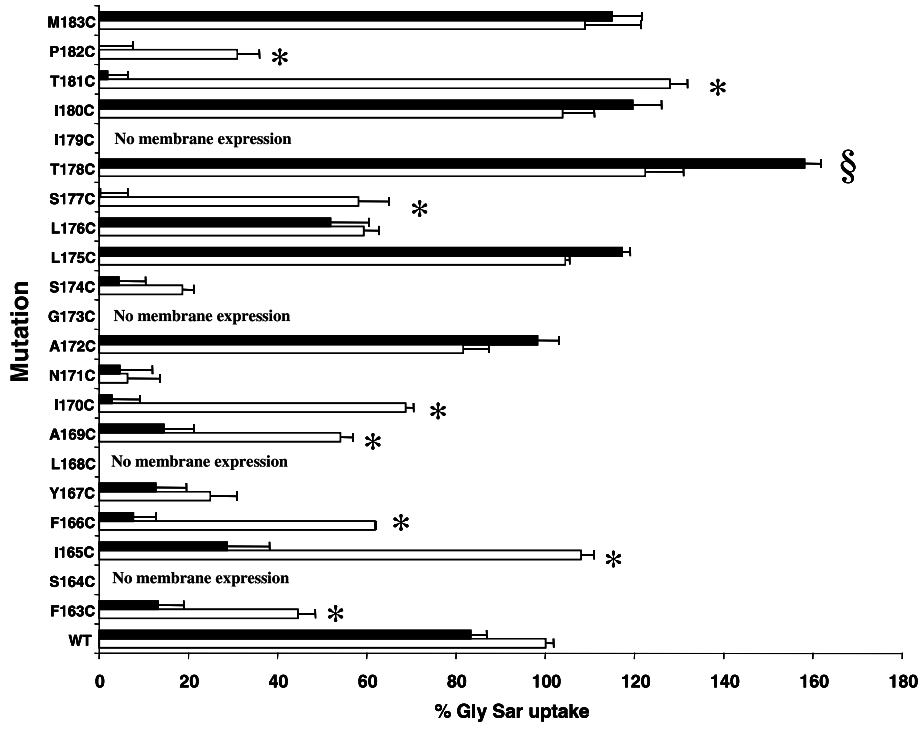

Fig. 5. Effect of 1 mM MTSET on [^{3}H]Gly-Sar uptake activities of the cysteine-scanning mutants of TMS5 of hPepT1. Seventy-two hours post-transfection, the transfected cells, adhered to the wells, were washed with the transport medium (Mes–Tris, pH 6, buffer). Each well was then incubated for 10 min at 37 °C with a solution containing [^{3}H]Gly-Sar (0.5 μCi/ml) after pre-incubation with 1 mM MTSET for 10 min. After washing thrice in ice-cold Mes–Tris (pH 6.0) buffer, the cells were lysed in 1 ml lysis buffer (1% SDS). BCA protein assay reagents were used to determine the protein content of each well and the cell-associated radioactivity was measured in a Beckman liquid scintillation counter. Results represent the % Gly-Sar uptake of each individual mutant transporter protein when compared with wild-type hPepT1 ($n = 4$–8). The background uptake values of mock-transfected HEK293 cells were subtracted. The white bars represent uptake activities in the absence of 1 mM MTSET and the black bars represent uptake activities in the presence of 1 mM MTSET. *, Highly significant inhibition of uptake activity by 1mM MTSET. §, Significant increase in uptake activity.

transport of the mutant proteins to the plasma membrane. This is not uncommon and single amino acid mutations have been previously shown to cause erroneous synthesis/trafficking in a variety of membrane proteins leading to very low expression levels [20,25].

Out of the 17 mutated transporters that were expressed correctly on the plasma membrane, Y167C-, N171C-, and S174C-hPepT1 were unable to tolerate the cysteine mutations at the corresponding amino acid residues. Y167 has already been shown to be crucial for hPepT1 activity [23]. Alanine mutation at N171 also abolished hPepT1 activity (unpublished results), leading to an increased confidence in our cysteine-scanning results. Interestingly, a helical wheel analysis of TMS5 suggests that these three amino acids are clustered together on one face of the putative α-helix formed by TMS5.

Preincubation with 1 mM MTSET resulted in a reduction in Gly-Sar uptake ($p < 0.05$) by the F163C-, I165C-, F166C-, A169C-, I170C-, S177C-, T181C-, and P182-hPepT1 transporters (Fig. 5). Inhibition of Gly-Sar uptake was complete and highly significant. Analysis of these data using a helical wheel model (Fig. 6) and using a three-dimensional α-helix model (Fig. 7) showed that the exofacial half of TMS5 formed a classical amphipathic helix with S174, S177, T181, and P182 clustered on one face (the solvent accessible face). The non-accessible residues formed the other face of the α-helix (the solvent inaccessible face). The cytoplasmic half of TMS5 does not follow the classical "amphipathic helix" model. Instead, all the cysteine mutations were apparently accessible to MTSET (Figs. 6 and 7), suggesting a crucial role for this half of TMS5 in hPepT1 activity. This is further supported by the presence of the obligatory amino acids Y167 and N171 in this portion of the α-helix. Overall, these results suggest that TMS5 lines the putative aqueous channel and is slightly tilted from the vertical axis of the channel, with the exofacial half forming a classical amphipathic α-helix and the cytoplasmic half being highly solvent accessible (Fig. 7).

Preincubation with 2.5 mM MTSEA produced the most dramatic reduction in Gly-Sar uptake activity for the F163C- and I170C-hPepT1 transporter proteins. F166C, L176C, S177C, T178C, I180C, T181C, and P182C also reacted with the 2.5 mM MTSEA, resulting in a decrease in uptake activity of these mutated

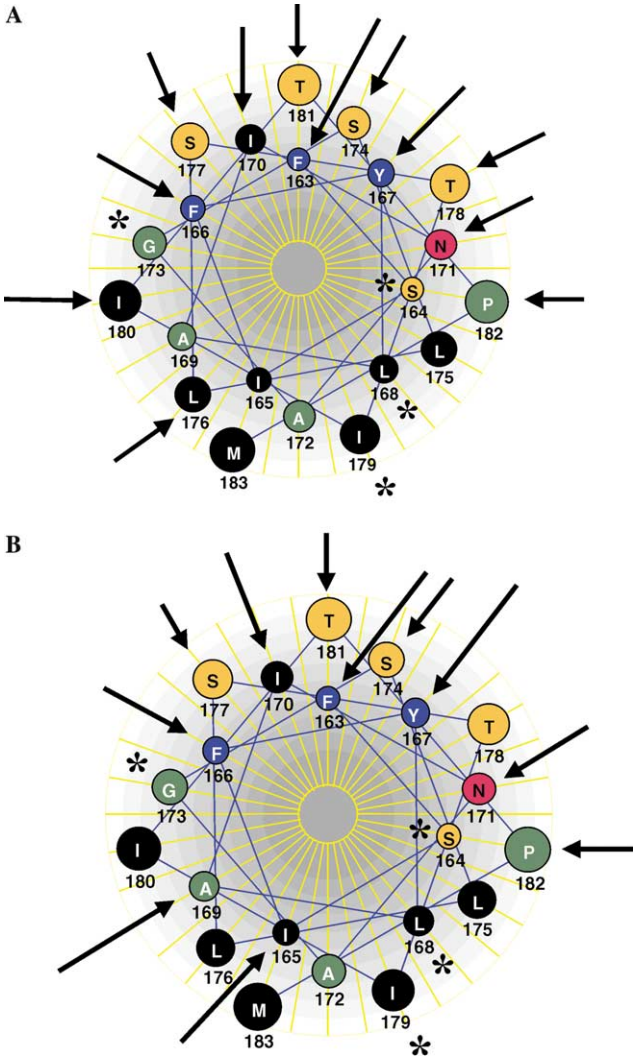

Fig. 6. Helical wheel model of TMS5 of hPepT1. Transmembrane segment 5 of hPepT1 as viewed from the extracellular side of the plasma membrane. Amino acids are represented by the single letter code and are colored based on their chemical properties. *, Cysteine substitutions at these residues resulted in mutant transporters that were unable to express on the plasma membrane of the HEK293 cells. (A) Arrows point to the residues that were unable to tolerate cysteine substitutions or were accessible to 2.5 mM MTSEA. (B) Arrows point to the residues that were unable to tolerate cysteine substitutions or were accessible to 1 mM MTSET.

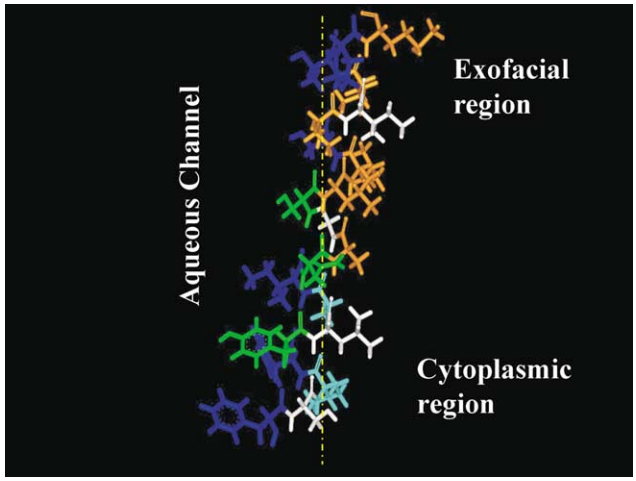

Fig. 7. Proposed orientation of TMS5 in hPepT1. A lateral view of TMS5 in hPepT1 with key transport amino acids (green), amino acids accessible to the MTS reagents (blue), those accessible only to MTSET (light blue), amino acids that hamper membrane expression when mutated to a cysteine (white), and non-accessible amino acids (orange). TMS5 lines the putative aqueous channel and is slightly tilted from the vertical axis (broken yellow line).

proteins, but to a much lesser extent. In contrast to MTSET, MTSEA has a greater degree of accessibility in the exofacial half of TMS5. This effect on some amino acids close to the exofacial surface can be attributed to its membrane-permeable nature. Hence, T178C and I180C react with MTSEA (Fig. 4) and their modification results in decreased Gly-Sar uptake. In contrast, these amino acids are inaccessible to MTSET (Fig. 5). S177C and T181C were reactive with MTSET and their modification eliminated Gly-Sar uptake (Fig. 5). These amino acids also react with MTSEA, but the effect on Gly-Sar uptake is smaller (Fig. 4). We attribute this to the smaller size of MTSEA (molecular volume = 66 $\AA^3$), compared to MTSET (molecular volume = 109 $\AA^3$). Since the inhibitory effect of the MTS reagents is primarily due to "physical blockade" of the aqueous pore, it may be that the pore is less efficiently blocked on the exofacial side by the smaller MTSEA reagent.

The relative sizes of MTSEA and MTSET may also be responsible for the different effects of modification by the two reagents in the cytoplasmic half of TMS5. In general, MTSEA modification of amino acids in this part of TMS5 has a much-reduced effect on Gly-Sar uptake, compared to MTSET (Figs. 4 and 5). However, modification by MTSEA at F163C and I170C produces a large reduction in Gly-Sar uptake (Fig. 4). F163 and I170 are positioned such that they protrude across the putative substrate channel (Fig. 7) and it may be that the channel in this region is relatively narrow, thus allowing the MTSEA-modified F163C and I170C to effectively block substrate transport.

Transmembrane helices possessing external solvent accessible faces that appear to line a part of their corresponding substrate permeation pathways have been demonstrated in a variety of proteins including the *E. coli* lac permease [26], glucose-6-P antiporter [27], Glut1 glucose transporter [19,25], metal-tetracycline/H^+ antiporter [21], and glutamate transporter [20]. For instance, TMS5 of the Glut1 glucose transporter is an amphipathic helix that possesses a solvent-accessible face lining a portion of its substrate permeation pathway. Helix 7 of the glucose-6-P antiporter and several helices within the lac-permease have been shown to possess solvent accessible faces that appear to line their respective substrate permeation pathways. It is impor-

tant to note that these proteins belong to the same 12 transmembrane helix superfamily of membrane transporters as hPepT1. Our finding that TMS5 of the dipeptide transporter hPepT1 shows a solvent accessible face lining the substrate translocation pathway fits into this structural paradigm.

Our data show that solvent accessibility of transmembrane segment 5 to the external aqueous environment occurs along its entire length. This is in contrast to the results for Glut1 where none of the five residues of transmembrane helix 5 predicted to lie closest to the cytoplasmic surface of the membrane displayed sensitivity to the sulfhydryl-specific reagent in the external solvent. Yan and Maloney [27] reported a similar result for helix 7 of the glucose-6-P antiporter. It should be noted that all our experiments were done at pH 6.0 when the protein is in its active state. Taking into account that hPepT1 needs protons for actively transporting substrates across the plasma membrane and combining this with the kinetic model described by Nussberger et al. [28], we propose a mechanism by which the binding of H^+ ions to a proton-binding site in hPepT1 causes a conformational change in the protein thereby exposing the solvent accessible residues along the entire length of transmembrane segment 5 to the substrate translocation pathway. Furthermore, we propose that Y167, N171, and S174 play a very critical role in the substrate binding as seen by the loss of activity of these mutated transporters. Similar studies on the other putative amphipathic transmembrane segments of hPepT1 will help in developing a critical understanding of the amino acids that line the substrate translocation pathway and may provide important clues regarding the substrate-binding site in the transporter.

Acknowledgments

This work was supported by the National Institutes of Health Grant GM59297 (V.H.L.L.). The authors thank Dr. Robert A. Farley of USC Department of Physiology for valuable suggestions. We also thank Michaela K. MacVeigh of the confocal microscopy subcore at the USC Keck School of Medicine Center for Liver Diseases (NIH IP30 DK48522), for her outstanding technical assistance.

References

[1] V. Ganapathy, G. Burckhardt, F.H. Leibach, Characteristics of glycylsarcosine transport in rabbit intestinal brush-border membrane vesicles, J. Biol. Chem. 259 (1984) 8954–8959.

[2] D.T. Thwaites, B.H. Hirst, N.L. Simmons, Substrate specificity of the di/tripeptide transporter in human intestinal epithelia (Caco-2): identification of substrates that undergo H(+)-coupled absorption, Br. J. Pharmacol. 113 (1994) 1050–1056.

[3] A. Tsuji, I. Tamai, H. Hirooka, T. Terasaki, Beta-lactam antibiotics and transport via the dipeptide carrier system across the intestinal brush-border membrane, Biochem. Pharmacol. 36 (1987) 565–567.

[4] U. Wenzel, D.T. Thwaites, H. Daniel, Stereoselective uptake of beta-lactam antibiotics by the intestinal peptide transporter, Br. J. Pharmacol. 116 (1995) 3021–3027.

[5] M. Boll, D. Markovich, W.M. Weber, H. Korte, H. Daniel, H. Murer, Expression cloning of a cDNA from rabbit small intestine related to proton-coupled transport of peptides, beta-lactam antibiotics and ACE-inhibitors, Pflugers Arch. 429 (1994) 146–149.

[6] D.T. Thwaites, M. Cavet, B.H. Hirst, N.L. Simmons, Angiotensin-converting enzyme (ACE) inhibitor transport in human intestinal epithelial (Caco-2) cells, Br. J. Pharmacol. 114 (1995) 981–986.

[7] K. Inui, Y. Tomita, T. Katsura, T. Okano, M. Takano, R. Hori, H+ coupled active transport of bestatin via the dipeptide transport system in rabbit intestinal brush-border membranes, J. Pharmacol. Exp. Ther. 260 (1992) 482–486.

[8] H. Han, R.L. de Vrueh, J.K. Rhie, K.M. Covitz, P.L. Smith, C.P. Lee, D.M. Oh, W. Sadee, G.L. Amidon, 5′-Amino acid esters of antiviral nucleosides, acyclovir, and AZT are absorbed by the intestinal PEPT1 peptide transporter, Pharm. Res. 15 (1998) 1154–1159.

[9] C.S. Temple, A.K. Stewart, D. Meredith, N.A. Lister, K.M. Morgan, I.D. Collier, R.D. Vaughan-Jones, C.A.R. Boyd, P.D. Bailey, J.R. Bronk, Peptide mimics as substrates for the intestinal peptide transporter, J. Biol. Chem. 273 (1998) 20–22.

[10] R. Liang, Y.J. Fei, P.D. Prasad, S. Ramamoorthy, H. Han, T.L. Yang-Feng, M.A. Hediger, V. Ganapathy, F.H. Leibach, Human intestinal H+/peptide cotransporter. Cloning, functional expression, and chromosomal localization, J. Biol. Chem. 270 (1995) 6456–6463.

[11] M.E. Ganapathy, W. Huang, H. Wang, V. Ganapathy, F.H. Leibach, Valacyclovir: a substrate for the intestinal and renal peptide transporters PEPT1 and PEPT2, Biochem. Biophys. Res. Commun 246 (1998) 270–275.

[12] P.J. Sinko, P.V. Balimane, Carrier-mediated intestinal absorption of valacyclovir, the L-valyl ester prodrug of acyclovir: 1. Interactions with peptides, organic anions and organic cations in rats, Biopharm. Drug Dispos. 19 (1998) 209–217.

[13] M. Sahin-Toth, H.R. Kaback, Cysteine scanning mutagenesis of putative transmembrane helices IX and X in the lactose permease of *Escherichia coli*, Protein Sci. 2 (1993) 1024–1033.

[14] J.A. Javitch, X. Li, J. Kaback, A. Karlin, A cysteine residue in the third membrane-spanning segment of the human D2 dopamine receptor is exposed in the binding-site crevice, Proc. Natl. Acad. Sci. USA 91 (1994) 10355–10359.

[15] Q. Lu, C. Miller, Silver as a probe of pore-forming residues in a potassium channel, Science 268 (1995) 304–307.

[16] M.T. Perez-Garcia, N. Chiamvimonvat, E. Marban, G.F. Tomaselli, Structure of the sodium channel pore revealed by serial cysteine mutagenesis, Proc. Natl. Acad. Sci. USA 93 (1996) 300–304.

[17] D. Fu, J.A. Ballesteros, H. Weinstein, J. Chen, J.A. Javitch, Residues in the seventh membrane-spanning segment of the dopamine D2 receptor accessible in the binding-site crevice, Biochemistry 35 (1996) 11278–11285.

[18] J.A. Javitch, L. Shi, M.M. Simpson, J. Chen, V. Chiappa, I. Visiers, H. Weinstein, J.A. Ballesteros, The fourth transmembrane segment of the dopamine D2 receptor: accessibility in the binding-site crevice and position in the transmembrane bundle, Biochemistry 39 (2000) 12190–12199.

[19] M. Mueckler, C. Makepeace, Transmembrane segment 5 of the Glut1 glucose transporter is an amphipathic helix that forms part of the sugar permeation pathway, J. Biol. Chem. 274 (1999) 10923–10926.

[20] D.J. Slotboom, W.N. Konings, J.S. Lolkema, Cysteine-scanning mutagenesis reveals a highly amphipathic, pore-lining membrane-spanning helix in the glutamate transporter GltT, J. Biol. Chem. 276 (2001) 10775–10781.

[21] N. Tamura, S. Konishi, S. Iwaki, T. Kimura-Someya, S. Nada, A. Yamaguchi, Complete cysteine-scanning mutagenesis and site-directed chemical modification of the Tn10-encoded metal-tetracycline/H+ antiporter, J. Biol. Chem. 276 (2001) 20330–20339.

[22] M.B. Bolger, I.S. Haworth, A.K. Yeung, D. Ann, H. von Grafenstein, S. Hamm-Alvarez, C.T. Okamoto, K.J. Kim, S.K. Basu, S. Wu, V.H. Lee, Structure, function, and molecular modeling approaches to the study of the intestinal dipeptide transporter PepT1, J. Pharm. Sci. 87 (1998) 1286–1291.

[23] A.K. Yeung, S.K. Basu, S.K. Wu, C. Chu, C.T. Okamoto, S.F. Hamm-Alvarez, H. von Grafenstein, W.C. Shen, K.J. Kim, M.B. Bolger, I.S. Haworth, D.K. Ann, V.H. Lee, Molecular identification of a role for tyrosine 167 in the function of the human intestinal proton-coupled dipeptide transporter (hPepT1), Biochem. Biophys. Res. Commun. 250 (1998) 103–107.

[24] V.H. Lee, C. Chu, E.D. Mahlin, S.K. Basu, D.K. Ann, M.B. Bolger, I.S. Haworth, A.K. Yeung, S.K. Wu, S. Hamm-Alvarez, C.T. Okamoto, Biopharmaceutics of transmucosal peptide and protein drug administration: role of transport mechanisms with a focus on the involvement of PepT1, J. Control. Release 62 (1999) 129–140.

[25] M. Mueckler, C. Makepeace, Analysis of transmembrane segment 10 of the Glut1 glucose transporter by cysteine-scanning mutagenesis and substituted cysteine accessibility, J. Biol. Chem. 277 (2002) 3498–3503.

[26] H.R. Kaback, J. Wu, From membrane to molecule to the third amino acid from the left with a membrane transport protein, Q. Rev. Biophys. 30 (1997) 333–364.

[27] R.T. Yan, P.C. Maloney, Residues in the pathway through a membrane transporter, Proc. Natl. Acad. Sci. USA 92 (1995) 5973–5976.

[28] S. Nussberger, A. Steel, D. Trotti, M.F. Romero, W.F. Boron, M.A. Hediger, Symmetry of H+ binding to the intra- and extracellular side of the H+-coupled oligopeptide cotransporter PepT1, J. Biol. Chem. 272 (1997) 7777–7785.